Applied Catalysis B: Environmental 180 (2016) 189–198

Contents lists available at ScienceDirect

Applied Catalysis B: Environmental

journal homepage: www.elsevier.com/locate/apcatb

A complete phenol oxidation pathway obtained during electro-Fenton treatment and validated by a kinetic model study

Emmanuel Mousset[a], Luigi Frunzo[b], Giovanni Esposito[c], Eric D. van Hullebusch[a], Nihal Oturan[a], Mehmet A. Oturan[a,*]

[a] Université Paris-Est, Laboratoire Géomatériaux et Environnement (LGE), EA 4508, UPEM, 77454 Marne-la-Vallée, France
[b] University of Naples Federico II, Department of Mathematics and Applications Renato Caccioppoli, Via Cintia, Monte S. Angelo, I-80126 Naples, Italy
[c] University of Cassino and the Southern Lazio, Department of Civil and Mechanical Engineering, Via Di Biasio, 43- 03043Cassino (FR), Italy

ARTICLE INFO

Article history:
Received 19 March 2015
Received in revised form 4 June 2015
Accepted 11 June 2015
Available online 19 June 2015

Keywords:
Aromatic compounds
Electrochemical advanced oxidation processes
Hydroxyl radical
Mathematical modelling
Oxidation by-products
Sensitivity analysis

ABSTRACT

A new approach of electro-Fenton modelling is proposed with phenol (PH) as a target contaminant. Five representative steps involved in the process have been considered: (i) H_2O_2 *in situ* generation, (ii) Fenton's reaction in bulk solution, (iii) Fe^{2+} (catalyst) electroregeneration, (iv) scavenging reactions (v) oxidative degradation and mineralization of PH as target pollutant. A new complete mineralization pathway of PH is proposed by gathering many intermediates that were found in different papers in literature and by adding some other ones to complete the oxidation route. A total number of 27 oxidation by-products of PH are considered, which represents 28 differential equations including PH. A sensitivity analysis of second-order kinetic parameters has been performed. It confirms the usefulness of the 49 kinetic reactions that have been taken into account and the importance of the five steps of the process, especially the fourth one. Based on existing parameter values found in literature, kinetic parameter estimations have been performed in order to better fit the experimental results. The model efficiency (ME), the root mean square error (RMSE) and the index of agreement (IoA) calculated to evaluate the performance of the model compared with experimental data have shown respectable values, which validate the model and the pathway. This model represents new understandings in mechanisms that occur during electrochemical advanced oxidation processes. It also improves the prediction of the concentration profiles of aromatic organic compounds and their intermediates.

1. Introduction

Hazardous and harmful compounds like phenol (PH) and its well-known by-products like hydroquinone (HQ) and para- benzoquinone (pBQ) are often found in wastewater mainly from petrochemicals industries, paint, pesticide, coal conversion [1] . Solutions containing many xenobiotics and especially aromatic compounds may undermine a biological process. Advanced oxidation processes (AOPs) have been developed as alternative technologies to conventional processes in recent decades [2,3] for treating recalcitrant pollutants. AOPs produce *in situ* hydroxyl radical (•OH), the strongest oxidizing agent (E° = 2.80 V/SHE, [4]) after fluorine. The latter is to be avoided because of its aggressivity in aqueous medium. These processes are especially efficient for aromatic molecules thanks to their non-selective electrophilic aromatic substitution of hydroxyl radical to aromatic moieties, leading finally to the ring opening reactions. Among AOPs, the emerging electro-Fenton process has shown promising results especially for industrial wastewaters treatment [5,6]. In contrast to the classical Fenton process, H_2O_2 is generated *in situ* at the cathode with O_2 or air feeding (Eqs. (1a)–(1d)) while an iron catalyst (Fe^{2+}, Fe^{3+}, or iron oxides) is added to the effluent to produce •OH at the bulk acidic solution *via* Fenton's reaction (Eq. (2)) [5,7]:

$$O_2 + e^- \rightarrow O_2^{\bullet -} \quad (1a)$$

$$O_2^{\bullet -} + H^+ \rightarrow HO_2^{\bullet} \quad (1b)$$

$$HO_2^{\bullet} + e^- \rightarrow HO_2^- \quad (1c)$$

$$HO_2^- + H^+ \rightarrow H_2O_2 \quad (1d)$$

$$Fe^{2+} + H_2O_2 + H^+ \rightarrow Fe^{3+} + H_2O + {}^{\bullet}OH \quad (2)$$

* Corresponding author.
E-mail address: Mehmet.oturan@univ-paris-est.fr (M.A. Oturan).

http://dx.doi.org/10.1016/j.apcatb.2015.06.014
0926-3373/

Fe^{2+} can then be electrocatalytically *in situ* regenerated mainly through Eq. (3) and secondly through Eqs. (4a) (4b) (4c):

$$Fe^{3+} + e^- \rightarrow Fe^{2+} \quad (3)$$

$$Fe^{3+} + H_2O_2 \leftrightarrow [Fe^{III}(HO_2)]^{2+} + H^+ \quad (4a)$$

$$[Fe^{III}(HO_2)]^{2+} \rightarrow Fe^{2+} + HO_2^{\bullet} \quad (4b)$$

$$Fe^{3+} + O_2^{\bullet -} \rightarrow Fe^{2+} + O_2 \quad (4c)$$

The aromatic compounds (ArH) can then be hydroxylated (Ar(OH)) through Eqs. (5a) and (5b):

$$ArH + {}^{\bullet}OH \rightarrow Ar(HOH)^{\bullet} \quad (5a)$$

$$Ar(HOH)^{\bullet} + O_2 \rightarrow Ar(OH) + HO_2 \quad (5b)$$

The hydroxylated compounds can then be oxidized in carboxylic acids (CA) following ring opening reactions through the following equation:

$$Ar + {}^{\bullet}OH/O_2 \rightarrow CA + CO_2 \quad (6)$$

Carboxylic acids thus formed can then be degraded in lower molecular weight CAs and finally mineralized to CO_2 as ultimate mineralization product:

$$CA1 + {}^{\bullet}OH/O_2 \rightarrow CA2 + CO_2 \quad (7a)$$

$$CA1, CA2, \ldots CA_n + {}^{\bullet}OH/O_2 \rightarrow CO_2 + H_2O \quad (7b)$$

The electro-Fenton process is considered as a clean treatment by minimizing the use of reagent and avoiding parasitic reactions without any production of sludge. Furthermore, the rate of organic pollutant removal as well as the mineralization yield are usually significantly higher than for classical chemical Fenton treatment [5].

Most of the kinetic models on AOPs have been proposed with UV/H_2O_2 treatment [8], classical Fenton process [9–16], Fenton-like treatment [17–19] and photo-Fenton process [20–22]. However, only two papers refer to electro-Fenton process [23,24]. Liu et al. [23] performed electro-Fenton in batch experiments and considered seven standard equations to model the evolution of H_2O_2 and the PH degradation by varying the concentration of initial Fe^{2+}, the oxygen concentration and the current density. Regalado-Mendez et al. [24] worked in continuously stirred tank reactor (CSTR) by using the same reactions as Liu et al. [23] for the model. Both studies simplified the model by not considering the oxidation by-products formed during the electrolysis, but only predict the PH concentration decrease.

However the prediction of the evolution of intermediates is also required since their toxicity can sometimes be even higher than the toxicity of the initial pollutant [25,26]. In the present study a new complete mineralization pathway of a representative pollutant such as PH treated by electro-Fenton is presented. This pathway describes the evolution of concentrations of intermediates like HQ, pBQ, catechol (CT), resorcinol (RS), maleic acid (MLE), fumaric acid (FUM), succinic acid (SUC), glyoxylic acid (GLYOX), oxalic acid (OXA) and formic acid (FOR). Sensitivity analysis and model validation by comparing model simulations with experimental data are then preformed.

2. Modelling

2.1. Steps involved in the electro-Fenton process

Fig. 1 highlights the 5 main groups of reactions involved in the electro-Fenton process, namely (i) H_2O_2 *in situ* generation, (ii) Fenton reaction in bulk solution, (iii) Fe^{2+} (catalyst) electroregeneration, (iv) scavenging reactions (v) oxidative degradation and mineralization of PH and its degradation. The developed model follows these 5 steps.

2.2. Assumptions

The assumptions made to establish the model are listed below:

- The adsorption of compounds and especially PH on carbon-felt cathode during the electro-Fenton treatment is considered negligible (less than 1% of adsorbed PH),
- The interferences from sulphate ion (SO_4^{2-}) and derivative species that could come from the electrolyte are considered negligible. The hydroperoxo iron complexes that could be formed [17] would not reduce the availability of iron since they can regenerate Fe^{2+} from Eqs. (4a)–(4c) [5],
- All the reactions were considered irreversible except the reactions between HQ and pBQ, between CT and oBQ and between MLE and FUM [27,28],
- No precipitation of iron(III) during experiment (low iron ion concentration and acidic medium) and the concentration of Fe^{2+} during the electrolysis was considered to be proportional to its initial concentration [23],
- The dissolved oxygen concentration ($[O_2]_{dissolved}$) is at saturation in the solution before starting the experiment and during the experiment, which permits to assume that $[O_2]_{dissolved}$ is constant during all the experiments [23] ,
- The concentration of H^+ and OH^- were considered constants, since the pH of the reaction medium remains constant during the experiments,
- The concentration of Fe^{2+} during the treatment was considered to be constant [23],
- The volume of reaction and the temperature of solutions were considered constant,
- The quasi-steady state approximation (QSSA) hypothesis was considered for hydroxyl radicals because they have very short half-time and are continuously produced and destroyed at a similar rate to attain a steady-state concentration in the bulk and/or the vicinity of the anode [5] ,
- The solutions are considered to be perfectly mixed and concentrations of compounds depend only on the treatment time,
- Polymerization, condensation, dimerization reactions were assumed to be negligible compared to the whole process of degradation by electro-Fenton [27].

2.3. Mass-balance equations

In batch experiments, the mass-balance equations can be determined according to the following equation:

$$\frac{dC_i}{dt} = R_i = \sum_n \nu r_{i,n} \quad (8)$$

where C_i is the molar concentration of compound i, $\nu_{i,n}$ is stoichiometric coefficient of compound i in reaction n, r_n is the reaction rate of reaction n and R_i is the production/consumption rate of compound i.

The chemical reactions selected to determine the pathway of PH during electro-Fenton treatment are represented in Table 1. There are 49 Reactions with 52 kinetic constants considered.

The matrix of equations used to elaborate the model is mentioned in Table SI-1 in supporting information. There are 30 differential equations and 1 algebraic equation that come from the QSSA of hydroxyl radical compound (Text SI-1 in supporting information). It represents 32 compounds that are considered including 4 inorganic compounds (H_2O_2, CO_2, Fe^{2+} and $^{\bullet}OH$) and 28 organic compounds (PH and its oxidation by-products).

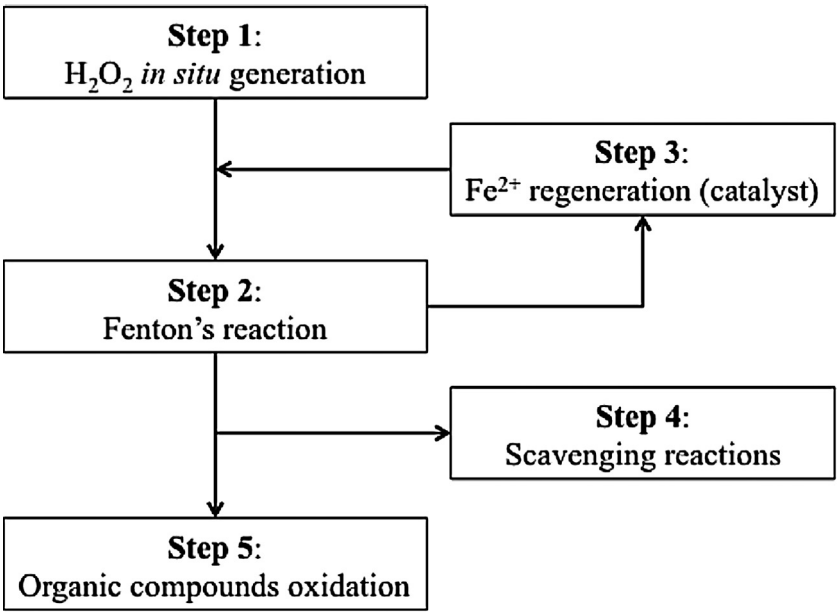

Fig. 1. Different steps involved during the electro-Fenton process.

2.4. Numeric integration

The simulations have been performed by original software developed in MATLAB® platform. The specific solver ODE15S multi-step was employed to solve the system of ordinary differential equations.

2.5. Sensitivity analysis

A sensitivity analysis for all the kinetic parameters used in the model was performed with AQUASIM® software in order to verify if all the parameters are influential and which of them are the most significant. The absolute relative (r) sensitivity function that measures the absolute (a) change in compound concentration (c) for a 100% change in the kinetic parameter (k) was used (Eq. (9)) [29]:

$$\delta_{c,k}^{a,r} = k\frac{\partial c}{\partial k} \tag{9}$$

2.6. Parameters estimation

Based on the available literature values, the guess values of the second order kinetic parameters were adjusted manually and refined by using FMINSEARCH tool of MATLAB®.

2.7. Model validation

In order to evaluate the fitting between experimental data and the suggested model, the model efficiency (ME), the root mean square error (RMSE) and the index of agreement (IoA) were calculated according to Eqs. (10)–(12), respectively [30]:

$$ME = 1 - \frac{\sum_{i=1}^{K}(y_i - y_i')^2}{\sum_{i=l}^{K}(y_i - y_m)} \tag{10}$$

$$RMSE = \sqrt{\frac{\sum_{i=l}^{K}(y_i - y_i')^2}{K}} \tag{11}$$

$$IoA = \frac{\sum_{i=l}^{K}(y_i - y_i')^2}{\sum_{i=l}^{K}(|y_i' - y_m| + |y_i - y_m|)^2} \tag{12}$$

where y_i is the single simulated value, y_i' is the corresponding observed value and y_M is the average of the simulated values.

3. Materials and methods

3.1. Chemicals

PH (>99.5%), HQ, RS, methanol (>99.9%, HPLC grade) and sodium sulfate were purchased from Aldrich. Heptahydrated ferrous sulfate ($FeSO_4{\cdot}7H_2O$), sulfuric acid and CT were supplied by Acros at analytical grade. Ultrapure water from a Millipore Simplicity 185 (conductivity < 6×10^{-8} S cm^{-1}) system was used in all experiments.

All the replicates of experiments and analyses gave standard deviations below 5%.

3.2. Batch tests of electro-Fenton process

Electro-Fenton experiments were performed in order to study the evolution of PH and its first detectable aromatic intermediates like HQ, CT and RS. The applied operating conditions were the same used by Pimentel et al. [27] to study the evolution of carboxylic acids formed during the oxidation of PH by electro-Fenton treatment.

Electrolysis experiments were performed in a 0.125 L undivided glass electrochemical batch reactor at current controlled conditions. The electrochemical cell was monitored by a power supply HAMEG 7042-5. The working electrode (cathode) was a 48 cm^2 carbon-felt piece (Carbone–Lorraine) and the counter electrode (anode), a platinum grid, was centred in the cell and surrounded by cathode covering the inner wall of the cell. A supporting electrolyte (Na_2SO_4 at 0.050 M) was added to the medium. $FeSO_4{\cdot}7H_2O$ was also added at 0.1 mM as catalyst (Fe^{2+}) source. Prior and during each experiment, the solutions were saturated in O_2 by supplying compressed air (0.25 L min^{-1}). All the solutions were stirred continuously by a magnetic stirrer. The pH of initial solutions was set at the optimal value of 3.0 (+/−0.1) by the addition of aqueous H_2SO_4

Table 1
Reactions involved in the electro-Fenton process and selected for the kinetic model.

#	Reaction	Reaction rates (r_n)
1	$O_2 + 2H^+ + 2e^- \xrightarrow{k_1} H_2O_2$	$r_1 = k_1 \frac{I}{A}$ [a]
2	$Fe^{2+} + H_2O_2 + H^+ \xrightarrow{k_2} Fe^{3+} + {}^\bullet OH + H_2O$	$r_2 = k_2 \left[Fe^{2+}\right] [H_2O_2]$
3	$Fe^{2+} + {}^\bullet OH \xrightarrow{k_3} Fe^{3+} + {}^-OH$	$r_3 = k_3 \left[Fe^{2+}\right] [{}^\bullet OH]$
4	$PH + {}^\bullet OH + O_2 \xrightarrow{k_4} CT + HO_2{}^\bullet$	$r_4 = k_4 [PH][{}^\bullet OH]$
5	$PH + {}^\bullet OH + O_2 \xrightarrow{k_5} HQ + HO_2{}^\bullet$	$r_5 = k_5 [PH][{}^\bullet OH]$
6	$PH + {}^\bullet OH + O_2 \xrightarrow{k_6} RS + HO_2{}^\bullet$	$r_6 = k_6 [PH][{}^\bullet OH]$
7a and b	$HQ + 2{}^\bullet OH + O_2 \overset{k_7/k_{-7}}{\leftrightarrow} pBQ + 2H_2O$	$r_7 = k_7[{}^\bullet OH]^2[HQ]$ $r_{-7} = k_{-7}[pBQ]$
8	$HQ + {}^\bullet OH + O_2 \xrightarrow{k_8} MUC + CO_2$	$r_8 = k_8[{}^\bullet OH][HQ]$
9	$HQ + {}^\bullet OH + O_2 \xrightarrow{k_9} MLE + CO_2$	$r_9 = k_9[{}^\bullet OH][HQ]$
10	$pBQ + {}^\bullet OH + O_2 \xrightarrow{k_{10}} MUC + CO_2$	$r_{10} = k_{10}[{}^\bullet OH][pBQ]$
11	$pBQ + {}^\bullet OH + O_2 \xrightarrow{k_{11}} MLE + CO_2$	$r_{11} = k_{11}[{}^\bullet OH][pBQ]$
12a and b	$CT + 2{}^\bullet OH \overset{k_{12}/k_{-12}}{\leftrightarrow} oBQ + 2H_2O$	$r_{12} = k_{12}[{}^\bullet OH]^2[CT]$ $r_{-12} = k_{-12}$ [oBQ]
13	$CT + 2{}^\bullet OH + O_2 \xrightarrow{k_{13}} PG + HO_2{}^\bullet$	$r_{13} = k_{13}[{}^\bullet OH][CT]$
14	$CT + {}^\bullet OH + O_2 \xrightarrow{k_{14}} MUC + CO_2$	$r_{14} = k_{14}[{}^\bullet OH][CT]$
15	$CT + {}^\bullet OH + O_2 \xrightarrow{k_{15}} MLE + CO_2$	$r_{15} = k_{15}[{}^\bullet OH][CT]$
16	$oBQ + {}^\bullet OH + O_2 \xrightarrow{k_{16}} MUC + CO_2$	$r_{16} = k_{16}[{}^\bullet OH][oBQ]$
17	$RS + {}^\bullet OH + O2 \xrightarrow{k_{17}} PG + HO_2{}^\bullet$	$r_{17} = k_{17}[{}^\bullet OH][RS]$
18	$PG + {}^\bullet OH + O_2 \xrightarrow{k_{18}} MUC + CO_2$	$r_{18} = k_{18}[{}^\bullet OH][PG]$
19	$PG + {}^\bullet OH + O_2 \xrightarrow{k_{19}} DHsBQ + CO_2$	$r_{19} = k_{19}[{}^\bullet OH][PG]$
20	$MUC + {}^\bullet OH + O_2 \xrightarrow{k_{20}} FUM + CO_2$	$r_{20} = k_{20}[MUC][{}^\bullet OH]$
21	$MUC + {}^\bullet OH + O_2 \xrightarrow{k_{21}} SUC + CO_2$	$r_{21} = k_{21}[MUC][{}^\bullet OH]$
22	$MUC + {}^\bullet OH + O_2 \xrightarrow{k_{22}} OBac + CO_2$	$r_{22} = k_{22}[MUC][{}^\bullet OH]$
23a and b	$MLE \overset{k_{23}/k_{-23}}{\leftrightarrow} FUM$	$r_{23} = k_{23}[MLE]$ $r_{-23} = k_{-23}[FUM]$
24	$MLE + {}^\bullet OH + O_2 \xrightarrow{k_{24}} OBac + CO_2$	$r_{24} = k_{24}[MLE][{}^\bullet OH]$
25	$FUM + {}^\bullet OH + O_2 \xrightarrow{k_{25}} OBac + CO_2$	$r_{25} = k_{25}[FUM][{}^\bullet OH]$
26	$FUM + {}^\bullet OH + O_2 \xrightarrow{k_{26}} SUC + CO_2$	$r_{26} = k_{26}[MLE][{}^\bullet OH]$
27	$SUC + {}^\bullet OH + O_2 \xrightarrow{k_{27}} PROP + CO_2$	$r_{27} = k_{27}[SUC][{}^\bullet OH]$
28	$OBac + {}^\bullet OH + O_2 \xrightarrow{k_{28}} GLYOX + CO_2$	$r_{28} = k_{28}[OBac][{}^\bullet OH]$
29	$PROP + {}^\bullet OH + O_2 \xrightarrow{k_{29}} CO_2 + H_2O$	$r_{29} = k_{29}[PROP][{}^\bullet OH]$
30	$GLYOX + {}^\bullet OH + O_2 \xrightarrow{k_{30}} CO_2 + H_2O$	$r_{30} = k_{30}[GLYOX][{}^\bullet OH]$
31	$DHsBQ + {}^\bullet OH + O_2 \xrightarrow{k_{31}} DHpBQ + CO_2$	$r_{31} = k_{31}[DH_sBQ][{}^\bullet OH]$
32	$DHpBQ + {}^\bullet OH + O_2 \xrightarrow{k_{32}} DHOac + CO_2$	$r_{32} = k_{32}[DH_pBQ][{}^\bullet OH]$
33	$DHOac + {}^\bullet OH + O_2 \xrightarrow{k_{33}} DHDac + CO_2$	$r_{33} = k_{33}[DHOac][{}^\bullet OH]$
34	$DHDac + {}^\bullet OH + O_2 \xrightarrow{k_{34}} DOB + CO_2$	$r_{34} = k_{34}[DHDac][{}^\bullet OH]$
35	$DOB + {}^\bullet OH + O_2 \xrightarrow{k_{35}} ACRac + CO_2$	$r_{35} = k_{35}[DOB][{}^\bullet OH]$
36	$ACRac + {}^\bullet OH + O_2 \xrightarrow{k_{36}} HPac + CO_2$	$r_{36} = k_{36}[ACRac][{}^\bullet OH]$
37	$HPac + {}^\bullet OH + O_2 \xrightarrow{k_{37}} GLYOX + CO_2$	$r_{37} = k_{37}[HPac][{}^\bullet OH]$
38	$HPac + {}^\bullet OH + O_2 \xrightarrow{k_{38}} OPac + CO_2$	$r_{38} = k_{38}[HPac][{}^\bullet OH]$
39	$OPac + {}^\bullet OH + O_2 \xrightarrow{k_{39}} MLO + CO_2$	$r_{39} = k_{39}[OPac][{}^\bullet OH]$
40	$MLO + {}^\bullet OH + O_2 \xrightarrow{k_{40}} TAR + CO_2$	$r_{40} = k_{40}[MLO][{}^\bullet OH]$
41	$TAR + {}^\bullet OH + O_2 \xrightarrow{k_{41}} ACE + CO_2$	$r_{41} = k_{41}[TAR][{}^\bullet OH]$
42	$TAR + {}^\bullet OH + O_2 \xrightarrow{k_{42}} KETO + CO_2$	$r_{42} = k_{42}[TAR][{}^\bullet OH]$
43	$KETO + {}^\bullet OH + O_2 \xrightarrow{k_{43}} OXA + CO_2$	$r_{43} = k_{43}[KETO][{}^\bullet OH]$
44	$ACE + {}^\bullet OH + O_2 \xrightarrow{k_{44}} OXA + CO_2$	$r_{44} = k_{44}[ACE][{}^\bullet OH]$
45	$ACE + {}^\bullet OH + O_2 \xrightarrow{k_{45}} FOR + CO_2$	$r_{45} = k_{45}[ACE][{}^\bullet OH]$
46	$ACE + {}^\bullet OH + O_2 \xrightarrow{k_{46}} CO_2 + H_2O$	$r_{46} = k_{46}[ACE][{}^\bullet OH]$
47	$OXA + {}^\bullet OH + O_2 \xrightarrow{k_{47}} FOR + CO_2$	$r_{47} = k_{47}[OXA][{}^\bullet OH]$
48	$OXA + {}^\bullet OH + O_2 \xrightarrow{k_{48}} CO_2 + H_2O$	$r_{48} = k_{48}[OXA][{}^\bullet OH]$
49	$FOR + {}^\bullet OH + O_2 \xrightarrow{k_{49}} CO_2 + H_2O$	$r_{49} = k_{49}[FOR][{}^\bullet OH]$

[a] where I is the current intensity and A is the surface of the electrode.

(1 M) solution. The pH variation was negligible and remained stable during all the experiment. PH was added at an initial concentration of 2.5 mM.

3.3. Analytical procedures

The decay of PH and aromatic by-products were followed by reversed phase liquid chromatography (HPLC) coupled with a UV-absorbance and a fluorescence detectors (Merck, Hitachi). A RP C-18 column placed in an oven and set at 40.0 °C was used. The mobile phase was a mixture of water + acetic acid (1%)/methanol (88:12 v/v) and the flow rate was set at 0.8 mL min^{-1}. Analyses were carried out at isocratic elution mode. The UV detection was carried out at 280 nm and the fluorescence detections were 250 and 350 nm for excitation and emission wavelengths, respectively. The injection volumes were 20 μL. The identification of the intermediates was performed by comparing the retention times with their respective standard solution injected in the same HPLC conditions.

4. Results and discussion

4.1. Sensitivity analysis

Sensitivity analysis for all the 52 kinetic parameters used in the model was performed. The influence of each parameter towards each compound is provided in Table 2, where parameters are ranked from the most to the least influential one. The respective graphs representing the compound sensitivity towards the kinetic parameter as a function of the treatment time are displayed in Fig. SI-1.

First of all, it has to be noted that all the kinetic parameters are more or less influential for at least one compound in the PH

Table 2
Sensitivity analysis of PH and its oxidation by-products regarding second-order kinetic parameter.

Compounds	Kinetic parameter impact on compound sensitivity
PH	$k_3 > k_1 > k_2 > k_4 > k_5$
CT	$k_3 > k_1 > k_2 > k_4 > k_{12} > k_5 > k_{14}$
HQ	$k_3 > k_1 > k_2 > k_7 > k_4 > k_8 > k_9 > k_{-7}$
RS	$k_3 > k_6 > k_{17} > k_1 > k_2 > k_4 > k_5$
MLE	$k_3 > k_1 > k_{24} > k_2 > k_{11} > k_{10} > k_5 > k_7 > k_4 > k_{15} > k_9 > k_8 > k_{12} > k_{23} > k_{20} > k_{22} > k_{-23} > k_{25} > k_{21} > k_{26}$
FUM	$k_3 > k_1 > k_{20} > k_{22} > k_{25} > k_2 > k_{21} > k_{26} > k_{23} > k_4 > k_{16} > k_{24} > k_{12} > k_5 > k_7 > k_{10} > k_{14} > k_8 > k_{15} > k_9$
SUC	$k_3 > k_{27} > k_1 > k_{22} = k_{21} > k_2 > k_{16} > k_{12} = k_4 > k_5 > k_{14} > k_8 > k_{10} > k_7 > k_{11}$
GLYOX	$k_3 > k_{30} > k_1 > k_2 > k_{21} > k_{22} > k_{28} > k_{16} > k_4 > k_{12} > k_5 > k_7 > k_{14} > k_8 > k_{10} > k_{11}$
OXA	$k_3 > k_1 > k_{48} > k_2 > k_{12} > k_{13} > k_{42} > k_{41} > k_{38} > k_{31} > k_{18} > k_{34} = k_{35} = k_{36} = k_{39} = k_{40} = k_{43} > k_{19} > k_{32} > k_6 > k_{33} > k_{17}$
FOR	$k_3 > k_1 > k_2 > k_{13} > k_{12} = k_{49} > k_{45} > k_{41} > k_{46} > k_{19} > k_{42} > k_{18} > k_{47} > k_{48} > k_{38} > k_4 > k_{31} > k_{37} > k_{40} > k_{36} > k_6 > k_{32} > k_{33} > k_{43}$

Table 3
Influence of the most important steps (and related kinetic parameters) on the sensitivity of PH and its oxidation by-products concentrations (Δconc. in percentage).

Compound	Δconc. with k_3 (%)	Δconc. with k_1 (%)	Δconc. with k_2 (%)	Δconc. with compound formation (%)	Δconc. with compound decomposition (%)
PH	30	−28	−18	–	−12 (k_4)
CT	31	−22	−14	14 (k_4)	−14 (k_{12})
HQ	30	−21	−11	14 (k_5)	−6 (k_7)
RS	68	−60	−35	73 (k_6)	−68 (k_{17})
MLE	40	−33	−16	17 (k_{11})	−33 (k_{24})
FUM	43	−30	−13	33 (k_{20})	−17 (k_{25})
SUC	40	−30	−12	24 (k_{21})	−36 (k_{27})
GLYOX	36	−24	−8	56 (k_{28})	−30 (k_{30})
OXA	25	−11	−4	1 (k_{43})	−11 (k_{48})
FOR	22	−8	−4	3 (k_{45})	−4 (k_{49})

mineralization pathway. Thus, this sensitivity analysis validates the role of the 49 kinetic reactions involved in the process. However, some kinetic parameters are more important than other ones as they are influential for all compounds evolution. The impact of the most important steps and the related kinetic parameters on the sensitivity of PH and its oxidation by-products concentrations are represented in Table 3. These values are exported from Fig. SI-1. Interesting information is that k_3 is the most influential parameter regarding all the compounds. It means that the 4th step of the process, *i.e.*, scavenging reaction between Fe^{2+} and •OH, is the most important one. The huge importance of this parasitic reaction is confirmed by other paper [5]. The concentrations increase for all compounds from 22% (FOR) to 68% (RS) with a 100% increase of k_3.

It is also highlighted that Reaction (1) (step 1) that represents the reduction of O_2 into H_2O_2 at the cathode is the 2nd most important in the process. The significance of this step makes a difference with classical Fenton models, since this reaction is specific for electrochemical processes.

Step 2 of the process, *i.e.*, Fenton reaction, is ranked at the 3rd place regarding the most influential parameter. This reaction has been reported to be high sensitive by Kang et al. [11] in Fenton model, since a 10% decrease of k_2 leads to an increase of 50% of the *p*- chlorophenol concentration. It has been shown by Pontes et al. [10] that a 50% decrease of k_2 results in increasing the PH concentration by 10% at the beginning of the Fenton treatment. It is similar to the present case, since PH concentration decreases by 18% when k_2 increases by 100%.

Moreover, for each compound the reactions that lead to their formation and decomposition have also an important role. They can have an impact of few percentages with FOR until around 70% with RS.

4.2. Kinetic parameter values used for simulation

In order to find a better fit for the simulated results with the experimental data the kinetic parameters were calibrated, after having tested their literature values. The average estimated values of the second order kinetic parameters are given in Table 4.

The estimated constant k_1 value ($1.7\ M^{-1}\ s^{-1}$) is similar to the one given by Liu et al. [23] that was $6.6\ M^{-1}\ s^{-1}$. The rate constant of Fenton's reaction is kept to $63\ M^{-1}\ s^{-1}$ as mentioned in several studies [5,10,11]. The high reactivity of •OH towards aromatic compounds is respected since the constant values from k_3 to k_{19} have range values between $10^8\ M^{-1}\ s^{-1}$ and $10^{10}\ M^{-1}\ s^{-1}$ [5,25,31,32]. For example, the estimated constant values of PH oxidation into CT, HQ and RS are 4.2×10^9, 3.47×10^9 and $5.09 \times 10^8\ M^{-1}\ s^{-1}$, respectively. These values are close to those proposed by Pontes et al. [10] with $3.3 \times 10^9\ M^{-1}\ s^{-1}$ for PH oxidation into CT and HQ. The constant value of PH oxidation into RS has not been found in the literature. However a lower constant value than with CT and HQ is consistent with the theory since the hydroxylation of PH having an activation group (—OH) on a benzene molecule is favoured in ortho (CT) and para (HQ) positions and in a less extend in meta (RS) position. As the medium is strongly oxidant, HQ is quickly oxidized to pBQ (high value of k_7) and then the latter is quickly oxidized into carboxylic acid (high k_8 value), which is in accordance with the literature [27].

The reactivity of •OH towards carboxylic acids shows estimated constants values between $10^6\ M^{-1}\ s^{-1}$ and $10^8\ M^{-1}\ s^{-1}$, which is in agreement with the ranges found in literature [28,33]. For example, the estimated constants values of ACE and FOR oxidation into CO_2 are $5 \times 10^7\ M^{-1}\ s^{-1}$ and $6.7 \times 10^7\ M^{-1}\ s^{-1}$, respectively, which are close to the values found in literature, *i.e.* $2.8 \times 10^7\ M^{-1}\ s^{-1}$ and $8.3 \times 10^7\ M^{-1}\ s^{-1}$, respectively [28].

4.3. Comparison between experimental data and simulated values

A large variety of representative compounds have been monitored during the electro-Fenton treatment of PH from the aromatic ones with 6 carbon atoms until formic acid with 1 carbon atom. Fig. 2 illustrates the comparison between simulated data and experimental data of PH decay and aromatic intermediates like HQ, CT and RS average evolutions during electro-Fenton treatment of PH.

Fig. 3 denotes the comparison between simulated data and experimental data of carboxylic acids average evolution (MLE, FUM, SUC, GLYOX, OXA, FOR) during electro-Fenton treatment of PH in

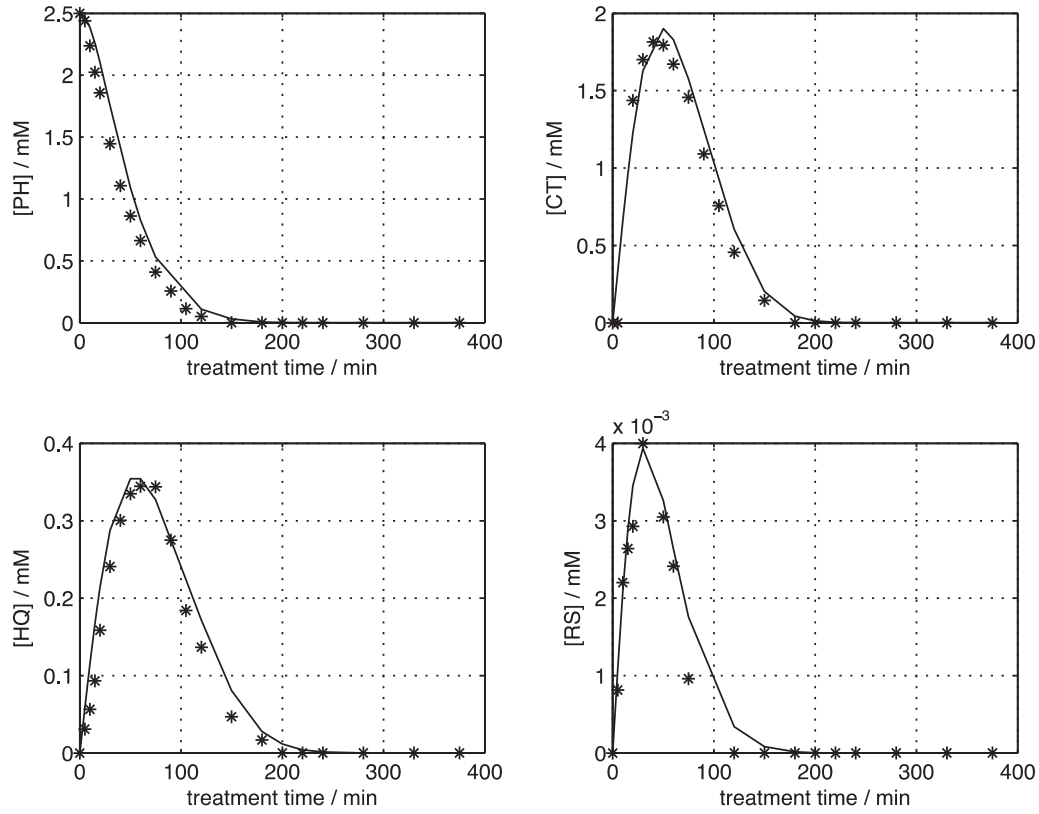

Fig. 2. Comparison of simulated (—) and experimental data (*) of PH decay and its aromatic intermediates (HQ, CT, RS) formed during an electro-Fenton treatment.

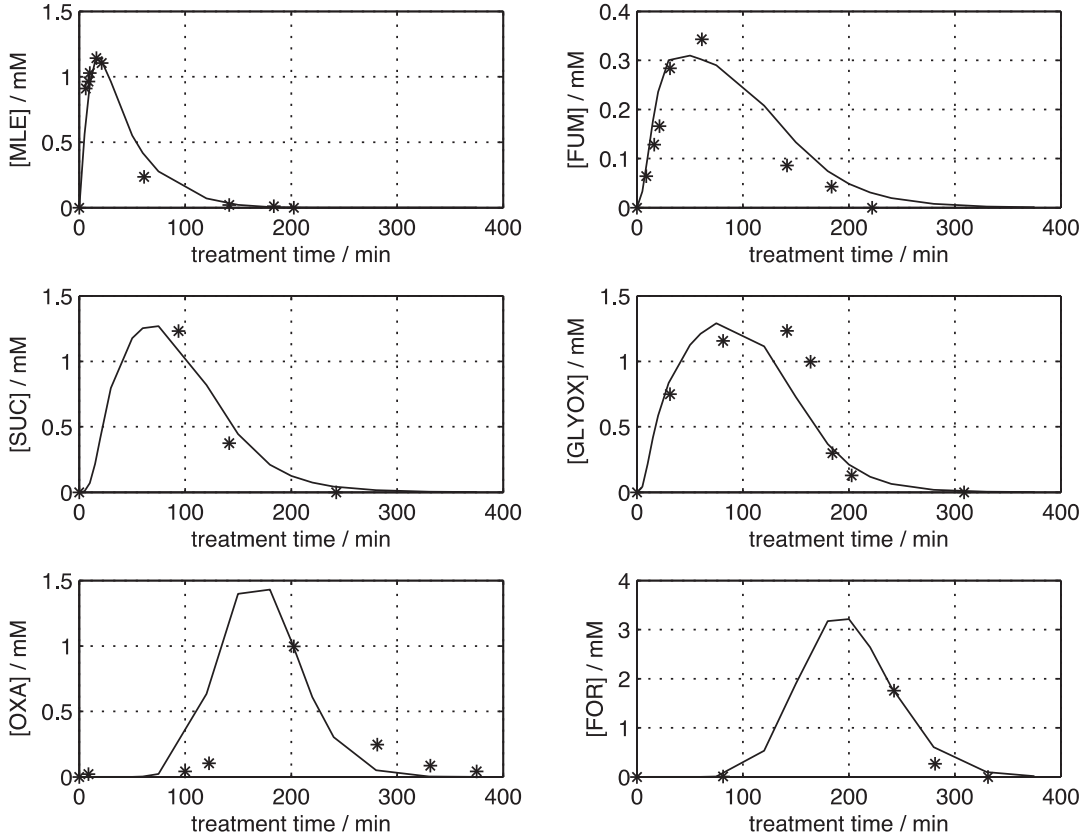

Fig. 3. Comparison of simulated (—) and experimental data (*) of carboxylic acids (MLE, FUM, SUC, GLYOX, OXA, FOR) formed during PH mineralization with electro- Fenton treatment.

Table 4
Estimated kinetic constants by assuming a second order kinetic model.

Kinetic constants	Kinetic constants values ($M^{-1}\ s^{-1}$)
k_1	1.7×10^0
k_2	6.3×10^1
k_3	5.0×10^9
k_4	4.2×10^9
k_5	3.5×10^9
k_6	5.1×10^8
k_7	6.0×10^9
k_{-7}	4.0×10^8
k_8	2.5×10^9
k_9	2.0×10^8
k_{10}	1.5×10^{10}
k_{11}	5.0×10^9
k_{12}	1.4×10^{10}
k_{-12}	9.0×10^5
k_{13}	1.0×10^8
k_{14}	4.0×10^8
k_{15}	5.0×10^7
k_{16}	2.5×10^9
k_{17}	1.5×10^{10}
k_{18}	5.0×10^9
k_{19}	4.0×10^{10}
k_{20}	2.7×10^7
k_{21}	3.4×10^8
k_{22}	6.0×10^8
k_{23}	2.7×10^7
k_{-23}	1.0×10^6
k_{24}	4.0×10^8
k_{25}	8.5×10^7
k_{26}	3.3×10^7
k_{27}	7.0×10^8
k_{28}	5.0×10^7
k_{29}	2.0×10^8
k_{30}	3.0×10^9
k_{31}	5.0×10^7
k_{32}	2.0×10^8
k_{33}	7.0×10^8
k_{34}	1.0×10^8
k_{35}	0.9×10^8
k_{36}	1.1×10^8
k_{37}	2.0×10^7
k_{38}	1.1×10^8
k_{39}	1.0×10^8
k_{40}	1.1×10^8
k_{41}	1.2×10^8
k_{42}	0.9×10^8
k_{43}	0.8×10^8
k_{44}	1.0×10^6
k_{45}	1.1×10^6
k_{46}	5.0×10^7
k_{47}	3.0×10^7
k_{48}	7.5×10^9
k_{49}	6.7×10^7

the same experimental conditions as Figs. 2 and 3 show a good fitting between experimental data and simulated values.

4.4. Model validation

Table 5 reports the average values of three parameters, *i.e.* ME, RMSE and IoA, with their respective standard deviations considering 3 simulations that permit to evaluate the performance of the model compared to the average experimental data. ME average values are higher than 0.98 (close to 1) for each monitored compound, except for FUM, GLYOX and OXA for which the values are around 0.97 (±0.0076), 0.96 (±0.0085) and 0.92 (±0.0104), respectively. It is also noted that RMSE average values are lower than 0.2 (close to 0) for each monitored compound, except for GLYOX and OXA for which the values are around 0.22 (±0.0054) and 0.23 (±0.0046), respectively. Moreover, IoA average values are higher than 0.99 (close to 1) for each monitored compound, except for FUM and OXA

Table 5
Model calibration and validation of PH and its oxidation by-products (standard deviations are represented in brackets).

	PH	CT	HQ	RS	MLE	FUM	SUC	GLYOX	OXA	FOR
ME	0.9991 ± 0.0005	0.9989 ± 0.0009	0.9978 ± 0.0012	0.9982 ± 0.0010	0.9945 ± 0.0017	0.9740 ± 0.0076	0.9868 ± 0.0056	0.9567 ± 0.0085	0.9239 ± 0.0104	0.9851 ± 0.0016
RMSE	0.1903 ± 0.0035	0.1691 ± 0.0010	0.0420 ± 0.0007	$3.4325 \times 10^{-4} \pm 0.0011 \times 10^{-4}$	0.1012 ± 0.0019	0.0464 ± 0.0005	0.0945 ± 0.0011	0.2220 ± 0.0054	0.2334 ± 0.0046	0.1465 ± 0.0023
IoA	0.9998 ± 0.0001	0.9997 ± 0.0002	0.9995 ± 0.0004	0.9996 ± 0.0002	0.9988 ± 0.0005	0.9683 ± 0.0132	0.9969 ± 0.0015	0.9913 ± 0.0022	0.9766 ± 0.0111	0.9966 ± 0.0014

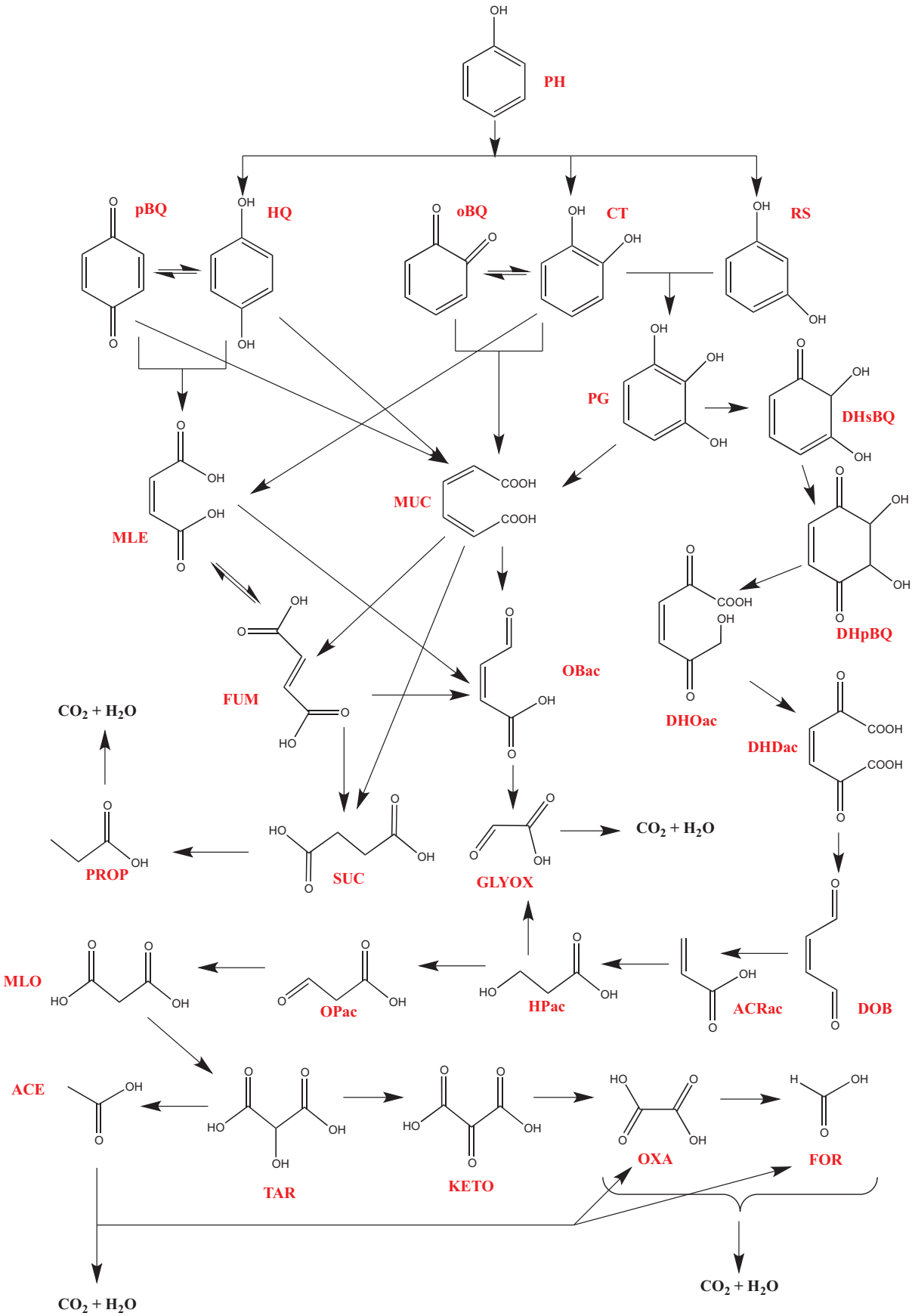

Fig. 4. Suggested complete PH mineralization pathways in acidic medium by hydroxyl radical generated by electro-Fenton process.

for which the values are around 0.97 (±0.0132) and 0.98 (±0.0111), respectively.

This shows that the model fits well the experimental data, as only one model could fit 10 compounds concentration profiles, thus validating the importance of the chemical kinetic reactions that have been considered in the present study.

4.5. Pathway of PH oxidation

The link between theory and experimental data permits to elaborate a complete mineralization pathway. The established model follows this pathway through the matrix of differential equations (Table SI-1) and has been applied and validated in previous subsections. Fig. 4 depicts the suggested pathway of PH mineralization by hydroxyl radicals formed through electro-Fenton process. The list of abbreviations of PH and its oxidation by-products is reported in Appendix A.

The degradation of PH into CT and HQ is widely suggested in former pathway of PH [27,34–37]. PH can also in a less extend be degraded into RS as observed in experiments and by other author [38]. Then equilibrium between HQ and pBQ and between CT and oBQ has been already suggested in literature [27]. The formation of PG through CT oxidation have been suggested by Pimentel et al. [27]. The formation of MLE through pBQ and CT oxidation has been suggested by Santos et al. [35]. The direct ring opening from hydroquinone was already highlighted [39]. The oxidations of CT, oBQ, HQ and pBQ into MUC have been already reviewed [38]. The formation of FUM from MUC was proposed by Zazo et al. [40]. The equilibrium between MLE and FUM has been proposed by many authors [27,28,38,40]. The indirect oxidation of MLE into SUC and then its oxidation into PROP and finally CO_2 have been suggested by Devlin and Harris [34]. The same authors have also proposed the indirect oxidation of MLE into GLYOX and then its oxidation into CO_2. The formations of DOB through DHDac oxidation and the oxidations of HPac into OPac and then into MLO have been proposed by the same authors [34]. Oturan et al. [28] have shown the possible pathways of oxidation of MLO into TAR and then into KETO and then into OXA. The indirect oxidation of MLE into ACE and the oxidation of OXA into FOR have been reported by Devlin and Harris [34]. The oxidation of ACE into OXA, FOR and CO_2 have been recommended by several authors [27,28].

Thus, this pathway is more accurate than the former ones since it contains more compounds, gathering information from several former described pathways and is validated by the model introduced in the present work.

5. Conclusions

A new electro-Fenton modelling approach is proposed with PH as a target pollutant. The sensitivity analysis, the kinetic parameter estimation and the validation of the model have demonstrated the suitability of the suggested pathway of PH degradation. The performance of fitting 10 compounds concentration profiles with only one model should be highlighted. In addition, this new achieved degradation/mineralization pathway of PH offers good perspectives regarding the understanding degradative mechanisms occurring during EAOPs treatment. Thus, the number of organic intermediate species that should be considered from aromatic compounds until ultimate carboxylic acids like OXA and FOR should be increased in established PH degradation pathways published in literature. This model also predicts the concentration profiles of several organic compounds, contributing to the development of EAOPs such as electro-Fenton process at larger scale. Further experiments and simulations should be done to evaluate the model in different conditions such as initial concentration of pollutant, Fe^{2+} concentration and current density.

Acknowledgements

The authors would like to thank the organizations that provided financial support: (i) The University of Paris-Est and (ii) theEuropean Commission through the Erasmus Mundus Joint Doctorate Programme ETeCoS^3(Environmental Technologies for Contaminated Solids, Soils and Sediments) under the grant agreement FPA no 2010-0009.

Appendix A.

List of abbreviations of PH and its oxidation by-products

ACE – Acetic acid
ACRac – Acrylic acid
CT – Catechol
DHDac – 2,5-dioxo-3-hexenedioic acid
DHOac – 2,5-dioxo-6-hydroxy-3-hexenoic acid
DHpBQ – 2,3-dihydroxy-1,4-benzoquinone
DHsBQ – 2,3-dihydroxy-semibenzoquinone
DOB – 1,4-dioxo-2-butene
FOR – Formic acid
FUM – Fumaric acid
GLYOX – Glyoxylic acid
HPac – 3-hydroxy-propanoic acid
HQ – Hydroquinone
KETO – Ketomalonic acid
MLE – Maleic acid
MLO – Malonic acid
MUC – Muconic acid
oBQ – Ortho-benzoquinone
OPac – 3-oxo-propanoic acid
OXA – Oxalic acid
pBQ – Para-benzoquinone
PG – Pyrogallol
PH – Phenol
PROP – Propanoic acid
RS – Resorcinol
SUC – Succinic acid
TAR – Tartronic acid

Appendix A. Supplementary data

Supplementary data associated with this article can be found, in the online version, at http://dx.doi.org/10.1016/j.apcatb.2015.06.014

References

[1] M. Ahmaruzzaman, Adv. Colloid Interface Sci. 143 (2008) 48–67.
[2] W.H. Glaze, J.W. Kang, D.H. Chapin, Ozone Sci. Eng. 9 (1987) 335–352.
[3] M.A. Oturan, J.-J. Aaron, Crit. Rev. Environ. Sci. Technol. 44 (2014) 2577–2641.
[4] W.M. Latimer, Soil Sci. 74 (1952) 333.
[5] E. Brillas, I. Sirès, M.A. Oturan, Chem. Rev. 109 (2009) 6570–6631.
[6] I. Sirés, E. Brillas, M.A. Oturan, M.A. Rodrigo, M. Panizza, Environ. Sci. Pollut. Res. Int. 21 (2014) 8336–8367.
[7] M.A. Oturan, J. Appl. Electrochem. 30 (2000) 475–482.
[8] X. Guo, D. Minakata, J. Niu, J. Crittenden, Environ. Sci. Technol. 48 (2014) 5718–5725.
[9] J.A. Zimbron, K.F. Reardon, Water Res. 43 (2009) 1831–1840.
[10] R.F.F. Pontes, J.E.F. Moraes, A. Machulek, J.M. Pinto, J. Hazard. Mater. 176 (2010) 402–413.
[11] N. Kang, D.S. Lee, J. Yoon, Chemosphere 47 (2002) 915–924.
[12] A. Santos, P. Yustos, S. Rodríguez, A. Romero, Catal. Today 151 (2010) 89–93.
[13] A. Santos, P. Yustos, S. Rodriíguez, F. Vicente, A. Romero, Ind. Eng. Chem. Res. 48 (2009) 2844–2850.

[14] J.A. Zazo, J.A. Casas, A.F. Mohedano, J.J. Rodriguez, Water Res. 43 (2009) 4063–4069.
[15] A.M. De Luis, J.I. Lombrana, A. Menendez, J. Sanz, Ind. Eng. Chem. Res. 50 (2011) 1928–1937.
[16] J. Anotai, M.-C. Lu, P. Chewpreecha, Water Res. 40 (2006) 1841–1847.
[17] J. De Laat, G. Le Truong, Environ. Sci. Technol. 39 (2005) 1811–1818.
[18] M.R. Rojas, F. Perez, D. Whitley, R.G. Arnold, A.E. Saez, Ind. Eng. Chem. Res. 49 (2010) 11331–11343.
[19] A. Bach, H. Shemer, R. Semiat, Desalination 264 (2010) 188–192.
[20] A. Cabrera Reina, L. Santos-Juanes Jordá, J.L. García Sánchez, J.L. Casas López, J.A. Sánchez Pérez, Appl. Catal. B Environ. 119–120 (2012) 132–138.
[21] H. Kusić, N. Koprivanac, A.L. Bozić, I. Selanec, J. Hazard. Mater. 136 (2006) 632–644.
[22] A. Babuponnusami, K. Muthukumar, Chem. Eng. J. 183 (2012) 1–9.
[23] H. Liu, X.Z. Li, Y.J. Leng, C. Wang, Water Res. 41 (2007) 1161–1167.
[24] A. Regalado- Méndez, E. Peralta-Reyes, M. Velazquez-Manzanares, Int. J. Comput. Scicence Inf. Technol. 2 (2010) 39–49.
[25] A. Dirany, I. Sirés, N. Oturan, A. Ozcan, M.A. Oturan, Environ. Sci. Technol. 46 (2012) 4074–4082.
[26] N. Oturan, S. Trajkovska, M.M.A. Oturan, M. Couderchet, J. Aaron, Environ. Pollut. 73 (2008) 1550–1556.
[27] M. Pimentel, N. Oturan, M. Dezotti, M.A. Oturan, Appl. Catal. B Environ. 83 (2008) 140–149.
[28] M.A. Oturan, M. Pimentel, N. Oturan, I. Sirés, Electrochim. Acta 54 (2008) 173–182.
[29] P. Reichert, Computer Program for the Identication and Simulation of Aquatic Systems, EAWAG (Switzerland) 1998. (http://www.eawag.ch/forschung/siam/software/aquasim/pdf/Reichert_1998_AQUASIM_Manual.pdf).
[30] G. Esposito, L. Frunzo, A. Panico, F. Pirozzi, Waste Manage. 31 (2011) 2527–2535.
[31] E. Mousset, N. Oturan, E.D. van Hullebusch, G. Guibaud, G. Esposito, M.A. Oturan, Water Res. 48 (2014) 306–316.
[32] M.A. Rodrigo, N. Oturan, M.A. Oturan, Chem. Rev. 114 (2014) 8720–8745.
[33] N. Oturan, E. Brillas, M.A. Oturan, Environ. Chem. Lett. 10 (2012) 165–170.
[34] H.R. Devlin, I.J. Harris, Ind. Eng. Chem. Fundam. 23 (1984) 387–392.
[35] A. Santos, P. Yustos, T. Cordero, S. Gomis, S. Rodríguez, F. García-Ochoa, Catal. Today 102–103 (2005) 213–218.
[36] R. Chen, J.J. Pignatello, Environ. Sci. Technol. 31 (1997) 2399–2406.
[37] X. Li, J.W. Cubbage, W.S. Jenks, J. Org. Chem. 64 (1999) 8525–8536.
[38] E.F. Mohamed, Removal of organic compounds from water by adsorption and photocatalytic oxidation, University of Toulouse (France) 2011. (http://ethesis.inp-toulouse.fr/archive/00001569/01/mohamed.pdf).
[39] X. Li, J.W. Cubbage, T.A. Tetzlaff, W.S. Jenks, J. Org. Chem. 64 (1999) 8509–8524.
[40] J.A. Zazo, J.A. Casas, A.F. Mohedano, M.A. Gilarranz, J.J. Rodríguez, Environ. Sci. Technol. 39 (2005) 9295–9302.